

# Chemical Vapor Deposition of Nickel Ferrite Using $\text{Ni}(\text{C}_5\text{H}_5)_2$ and $\text{FeC}_{14}\text{H}_{18}$

M. A. Kimbell

*Department of Electrical Engineering, Rose-Hulman Institute of Technology*

C.G. Takoudis

*Department of Chemical Engineering and Department of Bioengineering, University of Illinois at Chicago*

M. Singh and Y. Yang

*Department of Chemical Engineering, University of Illinois at Chicago*

Chemical vapor deposition was used to deposit a thin film of nickel oxide (NiO) and iron oxide ( $\text{Fe}_2\text{O}_3$ ) onto silicon substrates. Precursors chosen for this process were nickelocene ( $\text{Ni}(\text{C}_5\text{H}_5)_2$ ) and n-butylferrocene ( $\text{FeC}_{14}\text{H}_{18}$ ), which were oxidized with oxygen gas in a low-pressure reaction chamber. Following the deposition of the individual metal oxides, the two precursors were used together with the goal of depositing a thin film of nickel ferrite ( $\text{NiFe}_2\text{O}_4$ ). Both co-deposition and deposition in cycles were carried out, and the resulting thin films were analyzed using XPS. This research found that the resulting thin films did not contain  $\text{NiFe}_2\text{O}_4$ , but were composed of NiO and  $\text{Fe}_2\text{O}_3$  in a different ratio. It is suggested that changing various parameters in this experiment can be used to vary this ratio.

## Introduction

The magnetoelectric (ME) effect is exhibited by materials which are both ferromagnetic and ferroelastic. The coupling effect between these two properties causes the material to exhibit magnetization when subject to an external electric field, and electric polarization when subject to an external magnetic field.

The ME effect has been the subject of interest ever since its first demonstration over four decades ago.<sup>1,2</sup> However, a lack of understanding the causes of the effect on a molecular level, the scarcity of materials which demonstrate the ME effect, and the general weakness of the effect prevented it from being utilized in useful applications and led to a decline in research for quite some time.<sup>3</sup>

Recently there has been an arousal of interest due to the increased research of

magnetoelectric composite materials and methods for creating them. ME composite materials are made up of two or more layers consisting of a piezomagnetic (magnetostrictive) material and a piezoelectric (electrostrictive) material.<sup>4</sup> When a magnetic field is applied to the composite, the piezomagnetic material deforms and places stress on the piezoelectric material, which in turn generates an electric potential. Similarly, an applied electric field will cause the switching of magnetization. Potential applications of the ME effect include tunable microwave devices, sensors, and transducers.<sup>3</sup> The ME effect can also be used to make significant advancements in data storage by the utilization of multiple-state memory – by allowing data to be stored in an electric component as well as a magnetic component on a single media, the amount of

information that can be stored will drastically increase.<sup>5</sup>

One material of interest is nickel ferrite ( $\text{NiFe}_2\text{O}_4$ ).  $\text{NiFe}_2\text{O}_4$  is ferromagnetic and exhibits the magnetostrictive effect. If it can be deposited as a thin film reliably, it can be used as a novel way to create ME composite materials by deposition onto a piezoelectric substrate.

Chemical vapor deposition (CVD) is the process of depositing a solid material onto a heated substrate via a chemical reaction on the surface of the substrate from gas phase reactants. This paper deals with the deposition of  $\text{NiFe}_2\text{O}_4$  using CVD under low-pressure conditions for a variety of benefits, including purity and uniformity of thin films, and relative ease to perform in lab and reproduce results. Low-pressure CVD tends to reduce gas-phase reactions which can create particles in the air and cause defects on the thin film. It also allows for increased control over the stoichiometric ratios of reactant gases and is able to cover a large area without resulting in an uneven film thickness.

In CVD, chemical precursors are used as the source of the vapor which is transported into the reaction chamber – via a carrier gas – to react on the substrate. In this case, the carrier gas was argon. The precursors chosen for this experiment were nickelocene ( $\text{Ni}(\text{C}_5\text{H}_5)_2$ ), which has been used to deposit nickel oxide ( $\text{NiO}$ ) thin films<sup>6</sup> and n-butylferrocene ( $\text{FeC}_{14}\text{H}_{18}$ ), which has been used to deposit iron oxide ( $\text{Fe}_2\text{O}_3$ ) thin films.<sup>7</sup>

Data was individually taken on the deposition of  $\text{NiO}$  thin films and  $\text{Fe}_2\text{O}_3$  thin films. The temperature of the precursors and the temperature of the reaction chamber were varied. The precursor temperature varies the vapor pressure inside the precursor containers, which varies the amount of precursor delivered to the system. The reactor temperature controls the

temperature at which deposition occurs. Growth rates of the thin films were recorded under these various conditions in order to acquire the necessary conditions to deliver the correct stoichiometric ratio of the two precursors and deposit a thin film of  $\text{NiFe}_2\text{O}_4$ .

## Experimental

Silicon wafers of about 1 cm x 1 cm were used as substrates for depositing  $\text{Fe}_2\text{O}_3$  and  $\text{NiO}$  thin films. The wafers were cleaned with de-ionized water or acetone along with de-ionized water. They were then dried using nitrogen gas. The cleaned wafer was then loaded into a notched quartz boat to be loaded into the CVD system shown in Figure 1.

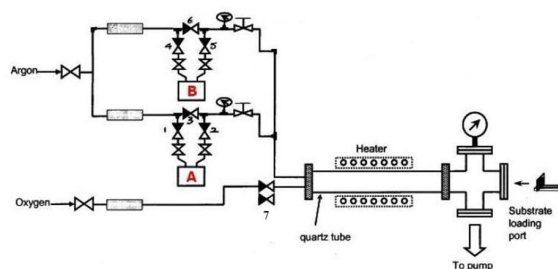


Figure 1 – Diagram of CVD System

Before loading the sample, the precursor container containing  $\text{Ni}(\text{C}_5\text{H}_5)_2$  or  $\text{FeC}_{14}\text{H}_{18}$  and the reaction chamber were heated using Omega temperature controllers. The precursor temperature ranged from 40°C to 70°C, and the reactor temperature was varied between 300°C and 600°C. The precursor delivery lines were heated to roughly 20°C above the temperature of the precursor using heating tape to prevent the precursor from condensing inside. The vacuum pump was then switched on and liquid nitrogen was added to a cold trap positioned between the vacuum pump and the system to trap byproduct particles and prevent the pump

from becoming clogged. The base pressure of the system in these conditions was 60 mTorr. The argon and oxygen valves were both opened and the gases allowed to flow, and the vacuum valve was closed, which allowed the pressure of the system to return to atmospheric pressure. The cleaned and prepared silicon wafer in the quartz boat was then loaded into the reaction chamber. To position the substrate in the same location in the reaction chamber consistently, it was always placed in the same slot on the quartz boat, and a marked rod was used to insert it a constant distance into the reaction chamber. The vacuum valve was opened again, causing the system to reach a pressure of 4 Torr. The CVD process was then run using a computer program written using LabVIEW software, which controlled various valves in the system. While CVD was being carried out, the pressure of the system was around 12 Torr. When the CVD process was completed, the LabVIEW program automatically closed the precursor valves and the system pressure returned to 4 Torr. The vacuum valve was then closed and the reactor depressurized, allowing the quartz boat and substrate to be removed.

The film thickness was measured using a spectral ellipsometer (J. A. Woollam Co., Inc. Model M-44). It was calibrated before each use with a silicon dioxide calibration standard. The thin film measurement was fit to a Cauchy distribution.

Using the data collected from NiO and Fe<sub>2</sub>O<sub>3</sub> thin films, NiFe<sub>2</sub>O<sub>4</sub> thin films were deposited. This was done using two different methods – alternating deposition of each metal oxide for a short period of time, and co-deposition of both metal oxides simultaneously.

For cycled deposition, the conditions used were 60°C nickelocene, 65°C n-butylferrocene, with a reactor temperature of 400°C. Cycles consisted of 60 seconds of NiO deposition

followed by 30 seconds of Fe<sub>2</sub>O<sub>3</sub> deposition, which was controlled by another labVIEW computer program. The experiment was run for 5 cycles. Another experiment was run under the same conditions but using much shorter cycles (12 seconds of NiO followed by 6 seconds of Fe<sub>2</sub>O<sub>3</sub> for 20 cycles).

Co-deposition was carried out using the same conditions as stated above (60°C nickelocene, 65°C n-butylferrocene, 400°C reactor). It was also carried out after lowering the temperature of the iron precursor to 60°C.

A summary of these experiments is shown in Table 1.

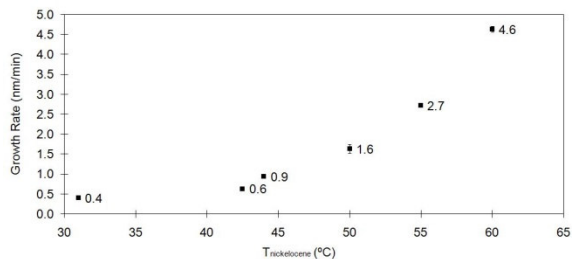
Sample #	Description
1	5 cycles 60 seconds NiO per cycle 90 seconds Fe <sub>2</sub> O <sub>3</sub> per cycle
2	20 cycles 12 seconds NiO per cycle 6 seconds Fe <sub>2</sub> O <sub>3</sub> per cycle
3	Co-deposition – 10 minutes 60°C nickelocene 65°C n-butylferrocene
4	Co-deposition – 10 minutes 60°C nickelocene 60°C butylferrocene

Table 1 – Summary of co-deposition and cycled deposition trials

The resulting thin films were then analyzed using x-ray photoelectron spectroscopy (XPS) to determine their chemical compositions.

## Results and Discussion

Figure 2 shows data taken on the growth rate of NiO with a constant reactor temperature of 400°C and varying precursor temperature.



**Figure 2 – Growth rate of nickel oxide as a function of precursor temperature (reactor temperature = 400°C)**

The graph in Figure 2 shows a trend of increasing growth rate with precursor temperature. The growth rate increases with increasing vapor pressure of nickelocene, which increases with temperature.

Figure 3 shows the growth rate of NiO with a constant precursor temperature of 50°C and varying reactor temperature.

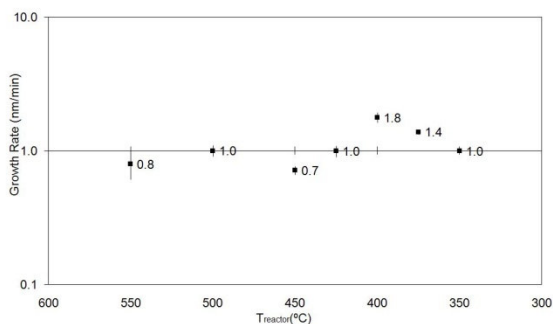


**Figure 3 – Growth rate of nickel oxide as a function of reactor temperature (precursor temperature = 50°C)**

There are two different mechanisms which control the growth rate of the thin film. The effects of these mechanisms can be seen in Figure 3. When the reaction is occurring at higher temperatures (550°C to 425°C), the temperature is high enough so that all or nearly all of the reactants which reach the substrate are able to react. When this is the case, the reaction is being limited by diffusion – the amount of reactants reaching the surface of the substrate. At lower temperatures (400°C to 350°C), it is easier for reactants to diffuse to the

substrate because of a thinner boundary layer. This means that at lower temperatures, the reaction is being limited by the amount of reactant gases available, and by the temperature of the reaction chamber, which decides how much of the reactant gases are allowed to react.

Figures 4 and 5 show similar graphs which illustrate the growth rate of Fe<sub>2</sub>O<sub>3</sub> on the substrate.

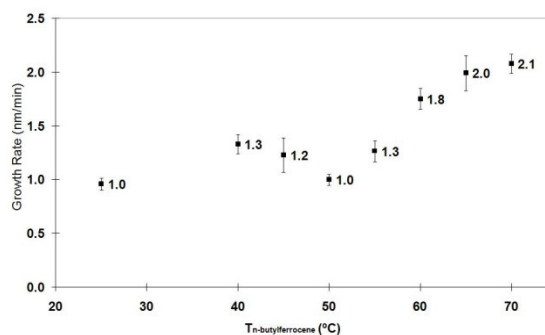


**Figure 4 – Growth rate of iron oxide as a function of precursor temperature (reactor temperature = 500°C)**

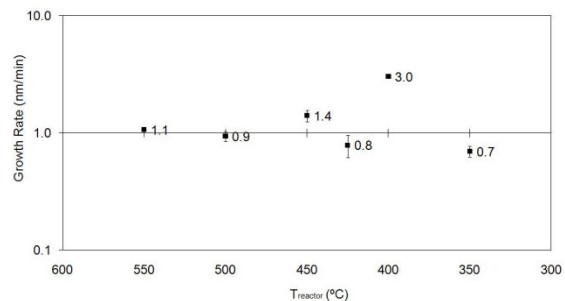


**Figure 5 – Growth rate of iron oxide as a function of reactor temperature (precursor temperature = 45°C)**

Figure 4 shows that Fe<sub>2</sub>O<sub>3</sub> thin films exhibit the same general trend of increasing growth rates with increasing precursor temperature, which is correlated to the vapor pressure of the n-butylferrocene precursor. Figure 5 shows both the section of the reaction limited by diffusion (reactor temperatures above 425°C), and the

section of the reaction limited by surface reaction kinetics (reactor temperatures below 425°C).

Co-deposition and cycled deposition was then carried out. XPS spectra for the four samples tested (see Table 1) are shown in Figure 6.

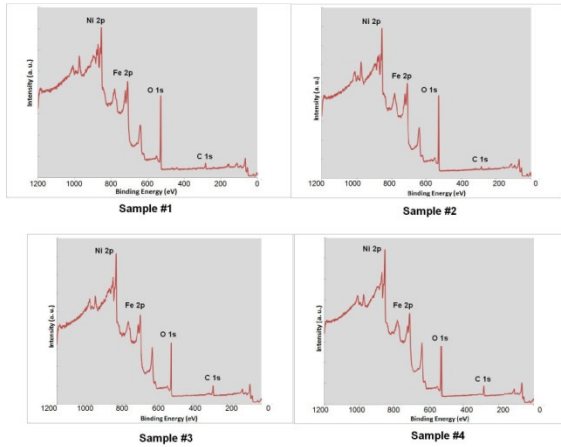


Figure 6 – XPS survey scans of samples 1-4

Analysis of this data showed that the thin films had the following compositions, shown in Table 2.

Sample #	Atomic Concentration (%)			
	Ni	Fe	O	C
1	23.13	27.30	37.31	12.27
2	24.82	28.81	39.40	6.97
3	26.50	22.69	30.29	20.52
4	29.17	22.11	31.07	17.65

Table 2 – Chemical composition of thin films from analysis of XPS data

In each case, the ratio of Ni to Fe is roughly one to one, which indicates that the thin films are not composed of  $\text{NiFe}_2\text{O}_4$ . XPS scans were also taken of specific bands of binding energies, corresponding to certain electron energy levels of each element in the thin films. This data was

used to identify the oxidation states of Ni and Fe in the films and further identify the composition of the material. The scans for Ni 2p and Fe 2p for Sample 1 are shown below in Figures 7 and 8.

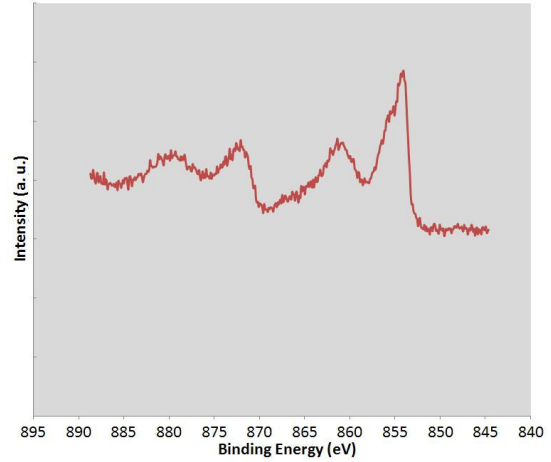


Figure 7 – Ni 2p region of XPS scan (Sample #1) – corrected to a carbon 1s peak of 284.5 eV

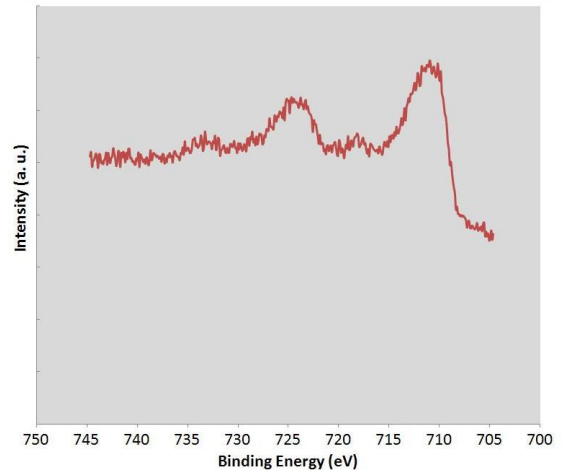


Figure 8 – Fe 2p region of XPS scan (Sample #1) – corrected to a carbon 1s peak of 284.5 eV

The location and shape of the peaks in the Fe 2p spectra correspond to the Fe(III) oxidation state, which indicates the presence of  $\text{Fe}_2\text{O}_3$ .<sup>8</sup> Similarly, the location and shape of the peaks in the Ni 2p spectra correspond to the Ni(II) oxidation state, which indicates the presence of  $\text{NiO}$ .<sup>9</sup> The same characteristics were observed

in the XPS spectra of Samples 2, 3, and 4. These are the results that were expected from previous research.<sup>6,7</sup> However, the metal-oxides are not in the correct ratio and did not form NiFe<sub>2</sub>O<sub>4</sub>.

A significant amount of carbon contamination was detected by XPS in the samples. Since argon sputtering was performed to remove contamination resulting from being exposed to the atmosphere, the presence of carbon in the thin films is most likely the result of precursor molecules that did not react. Raising the temperature of the reactor would cause more of the precursor molecules to react on the surface of the substrate and could reduce the amount of carbon in the thin films.

### Conclusions and Future Work

This research gathered data on the growth rates of NiO and Fe<sub>2</sub>O<sub>3</sub> thin films under numerous conditions. It has also found that by both co-deposition and deposition in cycles, n-butylferrocene and nickelocene can be used to deposit Fe<sub>2</sub>O<sub>3</sub> and NiO together in a single thin film. The future aim is to deposit both metal oxides together in the correct ratio to result in a thin film of NiFe<sub>2</sub>O<sub>4</sub>.

Future work for this project will include fine-tuning the conditions necessary to achieve this goal – this may include changing the temperature of the reactor and the temperatures of each precursor. Raising the reactor temperature may reduce the carbon contamination in the thin films, and tweaking the precursors' temperatures will adjust the stoichiometric ratios delivered to the reaction chamber.

Future work may also include using x-ray diffraction (XRD) to determine the crystalline structure of the thin films. The crystalline

structure will vary depending on the temperature of the deposition.<sup>10</sup> If the thin film of NiFe<sub>2</sub>O<sub>4</sub> is amorphous or contains defects in its crystalline lattice, adjustments in the reaction temperature or annealing at high temperatures may be required.

### Acknowledgements

The author would like to thank the National Science Foundation (NSF) and the Department of Defense (DoD) for providing funding for this research under EEC-NSF Grant # 0755115. The help received from Dr. Takoudis, Dr. Jursich, and graduate students Yi Yang, Manish Singh, and Qian Tao was also very much appreciated.

### References

- <sup>1</sup> E. Ascher, H. Rieder, H. Schmid, and H. Stössel, *J. Appl. Phys.* **37** (1966) 1404
- <sup>2</sup> W. Eerenstein, N. D. Mathur and J. F. Scott, *Nature* **442**, (2006) 759-765
- <sup>3</sup> M. Fiebig, *J. Phys. D: Apply. Phys.* **38** (2005) R123-R152
- <sup>4</sup> A.M.J.G. Van Run, D.R. Terrell, and J.H. Scholing, *Journal of Materials Science* **9** (1974) 1710-1714
- <sup>5</sup> Gajek, M. et al. Multiferroic tunnel junctions. Preprint at <http://arxiv.org/abs/cond-mat/0606444v1> (2006)
- <sup>6</sup> W. Yeh and M. Matsumura, *Jpn. J. Appl. Phys.* Vol. **36** (1997) Pt. 1, No. 11
- <sup>7</sup> M. Singh, Y. Yang, and C.G. Takoudis, *Journal of The Electrochemical Society*, **155** (9) (2008) D618-D623
- <sup>8</sup> S.A. Chambers, Y.J. Kim, and Y. Gao, *Surf. Sci. Spectra* **5** 219 (1998)
- <sup>9</sup> S. Oswald and W. Bruckner, *Surf. Interface Anal.* **36** (2004) 17–22
- <sup>10</sup> J. Kang and S. Rhee, *Thin Solid Films* **391** (2001) 57-61